JOURNAL OF AIRCRAFT
Vol. 45, No. 1, January–February 2008

Rotorcraft Parameter Identification from Real Time Flight Data

Rajan Kumar,* Ranjan Ganguli,† and S. N. Omkar‡
Indian Institute of Science, Bangalore 560 012, India
and
M. Vijaya Kumar§
Hindustan Aeronautics Limited, Bangalore 560 017, India

DOI: 10.2514/1.32024

Rotorcraft system identification involves the derivation of the model structure and parameters, such as aerodynamic stability and control derivatives, from flight-test results. Accurate rotorcraft system identification often requires higher order mathematical models. However, system identification becomes difficult and complicated as the number of modeling degrees of freedom are increased. In the present work, a new method for rotorcraft parameter estimation based on the application of a radial basis function network is proposed. The radial basis function network-based technique does not require a mathematical model of the helicopter, and the rotorcraft parameters can be directly computed from the flight data. The radial basis function network is found to give results in the same range as obtained from conventional parameter estimation techniques, such as the maximum likelihood method. Results obtained using the radial basis function network approach are compared to published research on the BO 105 helicopter and found to be in good agreement.

Nomenclature

a_i	=	Gaussian function
$f(x)$	=	generic function
$f(x)$	=	function approximation by the neural network
H	=	number of nodes in the hidden layer
L, M, N	=	moments about the x, y, and z axes
p, q, r	=	angular velocities about the x, y, and z axes
$\bar{r}$	=	number of patterns in the input layer
u, v, w	=	linear velocities along the x, y, and z axes
W_{im}	=	weight between the ith radial basis function unit and the mth output node
W_0	=	bias
X, Y, Z	=	forces along x, y, and z axes
x_{jt}	=	jth variable of the input pattern t
$\hat{x}_{jt}$	=	center of the ith radial basis function unit for the input variable j
y_{mt}	=	output of the mth node in the output layer for rth incoming pattern
α	=	noise level
ϵ	=	error norm
$\theta_0, \theta_{1c}, \theta_{1s}, \theta_{tr}$	=	control angles
σ_i	=	width of the ith radial basis function unit

Introduction

AERODYNAMIC stability and control parameters or derivatives are an integral part of a wide spectrum of applications such as piloted real time simulation, handling qualities analysis, and control system design. Different methods of aerodynamic derivative calculation for rotorcraft are available [1–3]. The aerodynamic parameters estimated using the system identification-based method are more accurate than the corresponding values predicted by other methods such as analytical and numerical differentiation [2,3]. This can be attributed to the use of flight-test data, which helps in removing the anomalies arising from assumptions and approximations made during modeling. The methodology of system identification is a process of reconstructing a simulation model structure and model parameters using experimental flight data by the application of a variety of techniques ranging from simple curve fitting algorithms to complex statistical error analysis. System identification has become a significant tool for applications such as model validation, handling qualities evaluation, control law design, and flight-vehicle design and certification [4].

The methodology and significance of system identification for flight vehicles is well documented [5–9]. The system identification method uses techniques such as the maximum likelihood method, equation error method, output error method, and filter error method. These methods require a mathematical model of the aircraft with a set of initial values for the parameters to begin the algorithm [10,11]. The identification methods are also affected by the presence of noise such as state noise or measurement noise [3]. The identification process becomes more difficult as the number of degrees of freedom (DOFs) and model parameters increase. This can be attributed to insufficient information content in the real time flight data [12]. These problems related to conventional parameter estimation techniques limit the inclusion of higher order DOFs in model development. However, higher order modeling is essential for nap of earth flight, aerial combats, high-g maneuvers, and the design of high-gain flight control systems [12,13].

New methods for aircraft parameter estimation aim to overcome the drawbacks of classical system identification methods. One such technique is the application of artificial neural networks (ANN) for parameter estimation [14–17]. The potential of ANN has already been shown in diverse fields such as nonlinear flight control, system identification, structural damage detection and identification, flight certification, failure rate prediction, and modeling complex phenomenon like ice accretion [18–29]. The neural networks are also used in a wide range of helicopter studies [30–32]. However, the flexibility of recurrent neural networks (RNN) in parameter

Received 8 May 2007; revision received 28 August 2007; accepted for publication 1 September 2007.

*Research Student, Department of Aerospace Engineering; rajank@aero.iisc.ernet.in.
†Associate Professor, Department of Aerospace Engineering; ganguli@aero.iisc.ernet.in. Senior Member AIAA.
‡Principal Research Scientist, Department of Aerospace Engineering; omkar@aero.iisc.ernet.in.
§External Ph.D. Student, Department of Aerospace Engineering; vijaym@aero.iisc.ernet.in.

estimation is limited because of the fixed number of neurons needed for state-space formulation [14]. In contrast, a feedforward neural network (FFNN) are capable of approximating any measurable function to any desired level of accuracy [33]. This property of the FFNN makes it an ideal choice for aircraft parameter estimation.

To avoid the drawbacks of conventional methods, two new neural network-based techniques, called the delta method and the zero method, were proposed by Raisinghani and his coworkers [15,16]. These methods do not require initial estimates of the parameters and the parameters can be directly extracted from the flight data. Raisinghani's approach has the ability to work as both an alternative and a complement to existing methods and also has the potential for online parameter estimation. These works are based on a type of FFNN known as the multilayer perceptron (MLP), which is popular in applications [26,34]. However, there are some drawbacks to using the MLP in realistic problems such as the slow convergence rate, computational memory, sensitiveness to outliers, etc. Such difficulties can be avoided by using a different type of FFNN known as the radial basis function network (RBFN) [34–36].

The aerodynamic derivatives estimated in previous works by Raisinghani et. al are from the simulated fixed wing data generated from decoupled lateral and longitudinal modes [15]. This modal decoupling is a reasonable assumption for a fixed wing aircraft, because the coupling between these modes is not significant. In the case of a rotary wing aircraft, lateral and longitudinal motions are strongly coupled due to the complex dynamics and aerodynamics. Therefore, the coupled equations of motion need to be used for generation of simulated data. Raisinghani et al. also suggested the removal of 25% of estimates from either end of the ordered set of estimates due to practical problems in parameter estimation in that region [16]. This has a serious implication on the helicopter studies, as it would severely affect both the transition and the high-speed flight regimes' characteristics. This drawback of the MLP-based delta method in derivative computation is overcome by the application of the RBFN in place of the MLP [37].

The objective of the present study is to establish a methodology for the computation of an aerodynamic derivative directly from flight data using the RBFN. The proposed methodology does not require a mathematical model of the rotorcraft. To the best of the authors' knowledge, this is the first such study in the field of rotary wing parametric estimation. In the present work, the delta method using the RBFN is first applied to simulated data with added measurement and state noise. The simulated data are generated by a 6-DOF nonlinear helicopter simulation model to include the coupled longitudinal and lateral modes. The established methodology is then applied for the derivative computation from BO 105 real time flight-test data. The results from the RBFN-based delta method are compared to the identified derivatives from the 6-DOF and 9-DOF models available in literature. In the present study, the modified 3211 pilot control input is used for rotorcraft parameter estimation. The estimated parameters are then verified from the data generated by a frequency sweep pilot control input for assessing the predictive capability of the RBFN-based delta method.

Radial Basis Function Neural Network

ANN is a nonlinear statistical data modeling tool that can be used to model complex relationships between input and output of the system. ANN can be broadly classified on the basis of the type of connectivity between neurons, the type of architecture, and the number of layers in the networks. FFNNs are composed of different layers of neurons, namely input layer, hidden layer(s), and output layer, in which each neuron is connected to others through weights. The training process of FFNNs is undertaken by changing the weights such that a desired input–output relationship is realized. There is a unidirectional flow of variables, making these networks static in nature. RNN are dynamic in nature as they have one or more feedback loops. More details on different types of ANN are available in [38].

The RBFN can be viewed as a curve fitting method in a high-dimensional space. The basic architecture of RBFN involves three

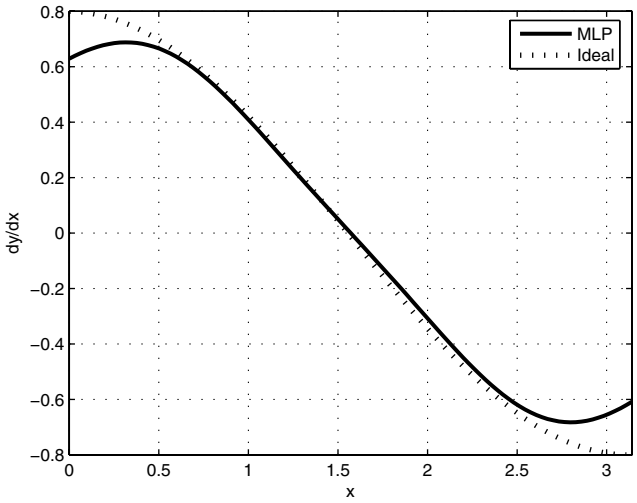

Fig. 1 Derivative computation of $y = 0.8 \sin x$ using the delta method and the MLP.

layers, as shown in Fig. 1. The input layer is made up of source nodes. The second layer is the hidden layer, which applies a nonlinear transformation from the input space to a high-dimensional hidden space. The third layer is made up of output neurons, which provide a linear transformation from the hidden space to the output space. The weights in RBFN are only present between the hidden layer and the output layer. RBFN is similar to the Gaussian density function which is defined by a center position and width parameter. The Gaussian density function gives the highest output when the input variables are at the center and decreases monotonically as the distance of the variables from the center increases. The batch mode k-means clustering algorithm is used for determining RBFN centers, and the weights between the hidden layer and output layer are trained by the linear least-squares optimization algorithm [38]. The k-means clustering algorithm finds a set of clusters with each dimensional center from the given training data. The dimensions of each center are determined by the number of input variables or input nodes. This cluster center becomes the center of the RBFN unit.

The overall input–output mapping can be denoted as follows:

$$y_{mt} = \sum_{i=1}^{H} W_{im} a_i(x_t) + W_0 \tag{1}$$

where the Gaussian function $a_i(x_t)$ is defined as follows:

$$a_i(x_t) = \exp\left[-\sum_{j=1}^{\bar{r}} \frac{[x_{jt} - \widehat{x_{ji}}]^2}{\sigma_i^2} \right] \tag{2}$$

Derivative Computation Using the Delta Method

The delta method is an artificial neural network-based method of parameter estimation. The derivative calculated using this method considers all the data points, thus introducing a smoothening effect in case of noisy data. The derivative calculation by neural network is given by

$$\left.\frac{\mathrm{d}y}{\mathrm{d}x}\right|_{x=x_i} = \frac{\hat{f}(x_1, \ldots, x_{i+1}, \ldots, x_n) - \hat{f}(x_1, \ldots, x_{i-1}, \ldots, x_n)}{2(x_{i+1} - x_{i-1})} \tag{3}$$

To calculate the derivative from the neural network, the network is first trained for a particular set of input–output values to create the approximate function $\hat{f}(x)$. Then, modified input files are prepared in which the variable about which the derivative has to be calculated is perturbed and the rest of the inputs are kept constant. These modified input files are then presented to the trained network, and corresponding predicted values of outputs are used for derivative calculation by the central difference technique. The aerodynamic

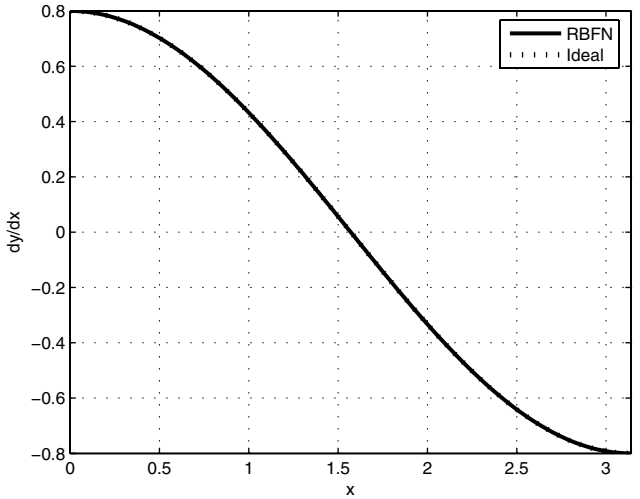

Fig. 2 Derivative computation of $y = 0.8 \sin x$ using the delta method and the RBFN.

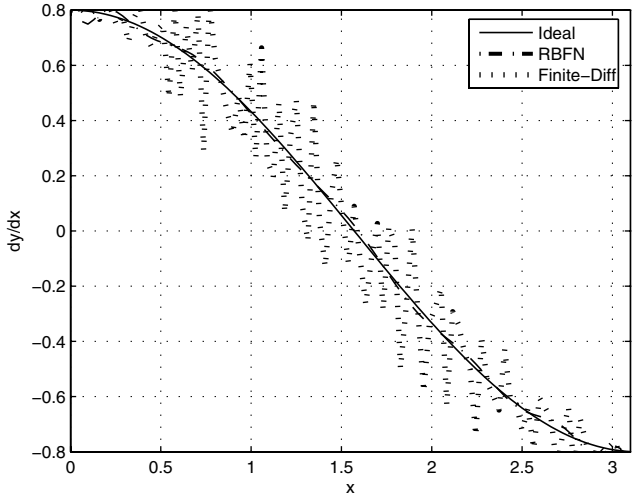

Fig. 3 Derivative computation and comparison of noisy data.

derivative calculation procedure for fixed wing aircraft is obtained from the literature [15,16]. The practical difficulties faced by Raisinghani et al. at the extremes is overcome by using RBFN in place of MLP.

Illustrative Example

The accuracy of the delta method is analyzed by applying it to a simple, single input–single output, nonlinear function given by Eq. (4). The data is generated for 100 points, of which 50 points are used for training and 50 points for testing of the neural network. Then the delta method is applied to both neural network architectures, namely, RBFN and MLP. The number of trainable parameters in both networks is kept the same to ensure a fair comparison. The derivative is calculated by both RBFN and MLP, and the results are compared to the analytical result given by Eq. (5). It can be seen from Fig. 1, that the MLP-based delta method is in error at the extremes. In contrast, the RBFN-based delta method is able to compute the derivatives more accurately over the whole range, as shown in Fig. 2.

$$y = 0.8 \sin x \qquad 0 \le x \le \pi \tag{4}$$

$$\frac{\mathrm{d}y}{\mathrm{d}x} = 0.8 \cos x \qquad 0 \le x \le \pi \tag{5}$$

The effect of the presence of noise in the simulated data on derivative computation is also analyzed for this simple single input–single output function given by Eq. (4). The noise in the simulated data is added as follows. Assuming that we have to include noise in a quantity Y, which is a vector of k elements, the Y_{noise} is obtained as follows:

$$Y_{\text{noise}} = Y[1 + (2\alpha R - \alpha)] \tag{6}$$

where α is the noise level and R is a vector of random numbers between 0 and 1 and has the same size as vector Y. The noise level in the present case is kept at 1%. The effect of noisy data on the derivative calculation can be seen in Fig. 3. It can be seen that, as expected, the finite difference technique gives a considerable amount of error when compared to the derivative computation with the help of the RBFN-based delta method. It can be seen from the illustrative example that the RBFN-based delta method is able to give better results at extremes of the data set compared to the MLP-based delta method. This property of the RBFN-based delta method makes it suitable for the rotorcraft parameter estimation as it enables the computation of aerodynamic parameters in both the transition regime and the high-speed flight regime that form the extremes of the forward speed variation. Also, we can deduce that the RBFN-based delta method gives satisfactory results when there is noise in the data, thus making it appropriate for the application of real time flight-test data, as it contains noise of varied levels and types.

Parameter Estimation Using Simulated Data

The 6-DOF nonlinear helicopter simulation model is based on the DLR, German Aerospace Center research BO 105, S123 helicopter. BO 105 is a lightweight, twin engine, multirole helicopter of 2.5 ton class belonging to the first generation of hingeless rotor helicopters. The simulation model used in this work is based on the level 1 model and subsystem modeling given by Padfield [2,39] and is coded in MATLAB 7.1.

Generation of Simulated Data

Simulated flight data for the computation of the quasi-steady derivatives are obtained from a 6-DOF nonlinear simulation model. The model is trimmed at various forward flight speeds, and the forces and moments are obtained at these trim points. The quasi-steady aerodynamic derivatives are then obtained using the central difference method by numerical perturbation of the state and control variables. The finite difference results are compared to the derivatives estimated using the RBFN-based delta method. The effect of state and measurement noise on both quasi-steady derivatives is studied by adding Gaussian noise of varying proportions to the simulated data.

Application of the RBFN-Based Delta Method to Simulated Data

The simulated data are generated for straight and level flight from a 6-DOF model. The rotorcraft model is trimmed at 70 speed points varying from 0–70 m/s, and various trim parameters are computed. The computed trim parameters are 1) trim control angles $(\theta_0, \theta_{1c}, \theta_{1s}, \theta_{tr})$, 2) trim forces (X, Y, Z), 3) trim moments (L, M, N), and 4) forward speed (u)

These parameters are then used for the derivative computation over a flight range of 0–70 m/s. The derivative computation is done by both the finite difference (FD) method and the RBFN-based delta method. The procedure of derivative computation using the RBFN-based delta method is enumerated stepwise and also shown in Fig. 4 using the Y_u stability derivative as an example:

1) The input file is made of trim control angles and forward speed.

2) The radial basis function network is then mapped with Y force as output.

3) Two different modified input data sets having $u \pm \Delta u$ are made, keeping the other variables constant.

4) The data set having $u + \Delta u$ is presented to the previously trained network and the perturbed output is Y^+.

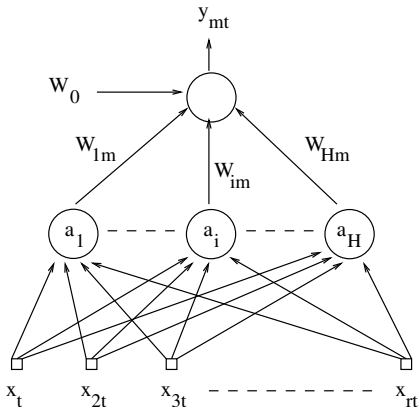

Fig. 4 Architecture of the radial basis function network (RBFN).

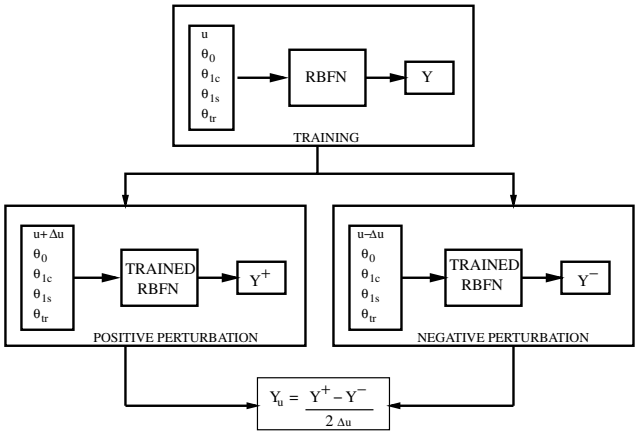

Fig. 5 Y_u schematic representation of derivative computation using the delta method.

5) Similarly, the data set having $u - \Delta u$ is presented to the trained network and the perturbed output is Y^-.

6) The Y_u derivative can now be computed as $[(Y^+) - (Y^-)]/2\Delta u$

The selection of the number of data points used for training is an important aspect in the RBFN-based delta method. In the present case, the training set consists of 35 data points. The testing set consists of 15 different data points.

The delta method is demonstrated by the computation of a few stability and control derivatives. The derivatives are selected, keeping in mind the nonlinearities and couplings involved, to show the ability of the RBFN in capturing these effects. The effect of the number of data points on the derivative computation is illustrated using the Y_u derivative computation in Figs. 5 and 6. In both cases, 35 data points are used for derivative computation using RBFN-based delta method. In Fig. 5, the finite difference technique uses the same 35 data points as used in the RBFN-based delta method. Figure 6 shows the result when the finite difference method uses all 70 points of the data set. Comparing Figs. 5 and 6, we can conclude that the finite difference technique requires a greater number of data points for better results. However, the RBFN-based delta method gives good results even when a lesser number of data points are used. Because flight-test data are expensive to obtain and available at few points, the RBFN can be used to obtain accurate derivatives in such cases.

The results are also analyzed and plotted for a 1% measurement noise and state noise level for stability derivatives and a 5% measurement noise and state noise level for control derivatives. Figure 7 shows the Y_u stability derivative at different forward speeds using noise free ideal data. Y_u is a coupled derivative type and the relatively high value of Y_u in low-speed flight can be attributed to the strong nonuniform inflow effects in this region. This nonuniform inflow effect diminishes with an increase in speed, thus making the value of Y_u tend toward zero. In the absence of noise, both the RBFN and FD derivatives match closely, showing that the neural network has been properly trained. The effect of measurement and state noise on the Y_u derivative computation is shown in Fig. 8. The RBFN is satisfactorily able to compute the derivative, whereas the FD gives

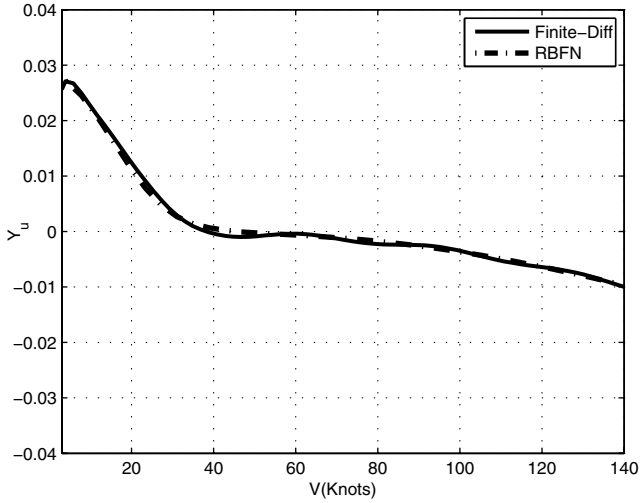

Fig. 6 Y_u stability derivative calculated using the radial basis function network and the finite difference method for 35 data points.

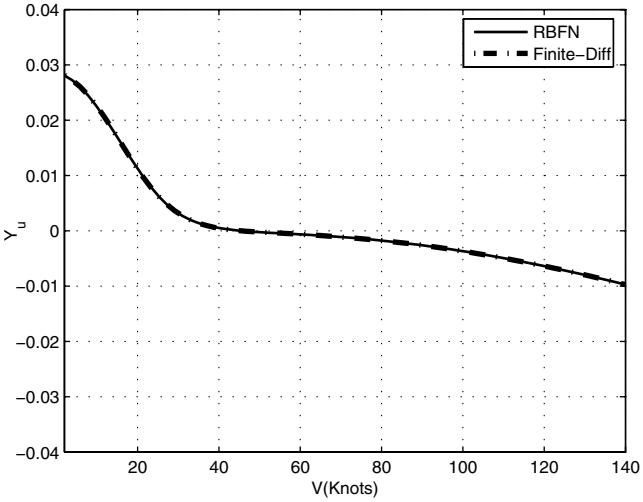

Fig. 7 Y_u stability derivative calculated using the radial basis function network and the finite difference method for ideal (zero noise) data.

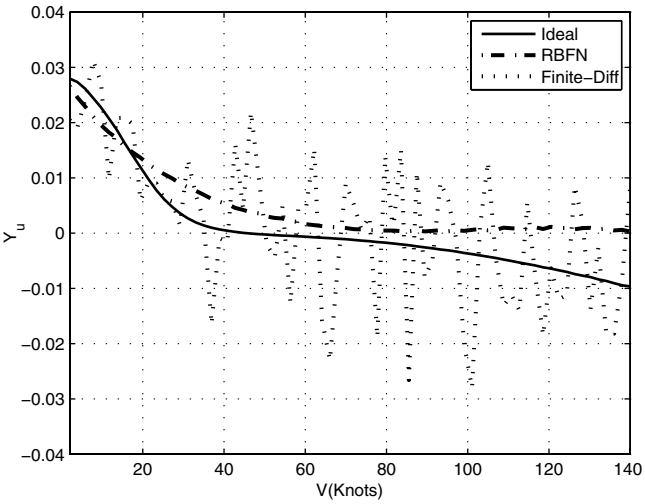

Fig. 8 Y_u stability derivative calculated using ideal (zero noise, finite difference) and noisy data.

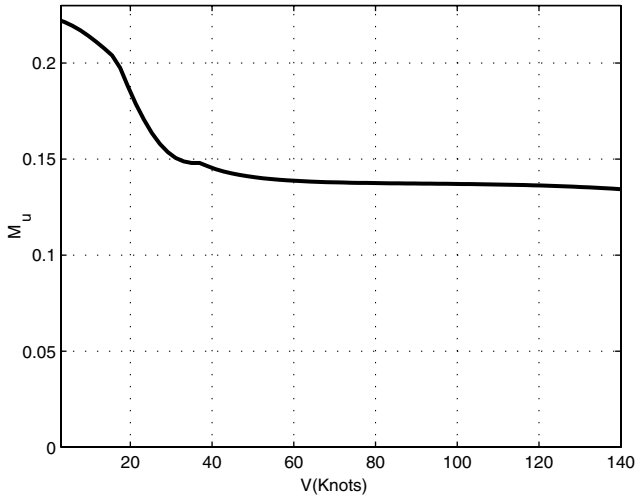

Fig. 9 M_u stability derivative calculated using ideal (zero noise) data.

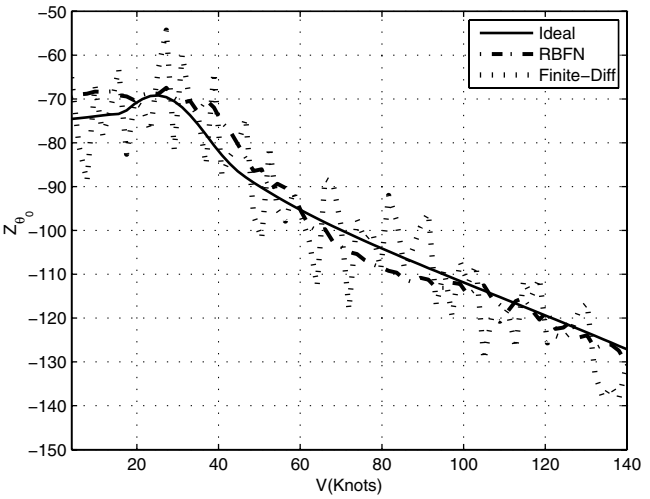

Fig. 11 Z_{θ_0} control derivative calculated using ideal (zero noise, finite difference) and noisy data.

considerable errors. Using the aforementioned methodology, the static speed derivative M_u is computed and illustrated in Fig. 9.

The Z_{θ_0} control derivative computation using the RBFN is shown in Fig. 10. The Z_{θ_0} is an important control derivative as it gives the heave control sensitivity and affects the heave response to the pilot's main rotor collective input. The RBFN is successfully able to compute the control derivative and gives results similar to those obtained from the FD in the case of ideal data. As shown in Fig. 11, the presence of noise in the data severely affects the derivative computation using the FD, but the RBFN gives results which closely match the ideal case.

The derivatives results are also presented in a tabular form in Tables 1 and 2 to show the effect of different noise levels on the derivative computation by both the finite difference method and the RBFN. The same levels for both state and measurement noise is used in the comparisons. The comparison has been made using an error norm between the numerical FD and RBFN outputs in the case of both simulated and noisy data. The derivative obtained from noisy data by both the FD and RBFN techniques is compared to the value of the derivative computed by the FD method from the simulated data having no noise. The error norm is defined as follows:

$$\epsilon_{X_u} = \sqrt{\frac{\|\hat{X}_{u,\alpha} - X^{\mathrm{FD}}_{u,\alpha=0}\|}{\|X^{\mathrm{FD}}_{u,\alpha=0}\|}} \tag{7}$$

where X denotes any general force and moment and u is a general state or control variable. $\hat{X}_{u,\alpha}$ is the value of the derivative calculated from either the FD or RBFN methods at a particular noise level α. The comparison between the RBFN and FD for the Y_u stability derivative is shown in Table 1. The error in the derivative calculation by the FD increases steadily with an increase in the noise level in the simulated data whereas the RBFN gives satisfactory outputs at the higher noise levels. Table 2 compares the RBFN and FD results for the Z_{θ_0} control derivative.

In summary, we see that the quasi-static derivatives can be calculated accurately using the delta method based on the RBFN. For the ideal or zero noise case, the delta method matches almost exactly with the finite difference method. Furthermore, the delta method using the RBFN does not give any problems at the extreme flight conditions that have been observed with the MLP. Finally, we note that when the simulated data are contaminated with state and measurement noise, the RBFN is better able to compute the derivatives, whereas the finite difference method amplifies any noise in the data.

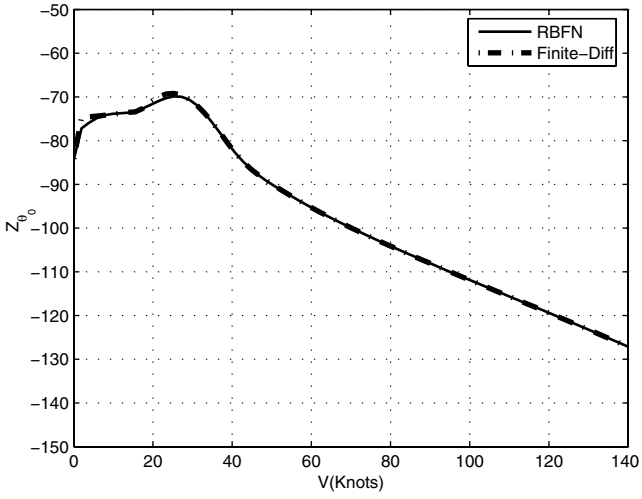

Fig. 10 Z_{θ_0} control derivative calculated using the radial basis function network and the finite difference method for ideal (zero noise) data.

Parameter Estimation Using BO 105 Flight Data

The parameter estimation from real time flight-test data is a complex process. Conventional parameter estimation techniques such as the maximum likelihood estimator require a mathematical model of the system. The values of unknown parameters are determined by exciting the system by suitable input and then

Table 1 Error in the Y_u derivative for simulated data with different noise levels

Noise level α, %	Delta method	Finite difference method
0	0.2260	0
1	0.3953	1.4016
3	0.6502	4.3485
5	0.7638	7.7113
7	0.8737	9.7445
10	1.0393	14.9452

Table 2 Error in the Z_{θ_0} derivative for simulated data with different noise levels

Noise level α, %	Delta method	Finite difference method
0	0.1043	0
1	0.1159	0.1388
3	0.1485	0.2789
5	0.1611	0.3057
7	0.1981	0.3481
10	0.2172	0.4424

Table 3 Computational parameters used in the RBFN-based delta method

Serial no.	Computational parameters	Value
1	Number of neurons	234
2	Spread of radial basis function	10–35
3	Δu	0.001 m/s
4	Δv	0.001 m/s
5	Δw	0.001 m/s
6	Δp	0.0001 rad/s
7	Δq	0.0001 rad/s
8	Δr	0.0001 rad/s
9	$\Delta\theta_0$	0.0001 rad
10	$\Delta\theta_{1c}$	0.0001 rad
11	$\Delta\theta_{1s}$	0.0001 rad

measuring the input and actual system response. The values of unknown parameters are then computed based on the requirement that the response of the model to a given input matches with the actual response. These model-based methods become more complicated in the presence of measurement and state noise. Higher order modeling also makes the identification process difficult, as the number of parameters increase. The RBFN-based delta method does not require any mathematical modeling and the parameters can be computed directly from flight data.

BO 105 Flight-Test Database

Flight tests with BO 105 S123 were conducted by the DLR, German Aerospace Center in 1987 for system identification and simulation validation purposes. These flight tests are briefly described next, because data from them are used in this paper to test the RBFN-based delta method. Trim condition was steady-state horizontal flight of 80 m/s at a density altitude of 915 m. The flight-test data consist of measurements that include linear and angular acceleration components, angular rates, linear velocity components, control inputs at the pilot's stick and rotor blades, along with other variables. The pilot inputs used in the flight tests were 1) positive and negative doublet inputs for each control variable, 2) positive and negative modified 3211 inputs for each control variable, and 3) pilot generated frequency sweeps for each of the four controls.

These inputs were applied to each control individually and the other three controls were kept fixed at their trim values. This was done to avoid correlation errors and to excite on-axis response. For the test inputs' specifications and other details, the reader is referred to the work by Fu and Kaletka [12]. The doublet test input is capable of exciting modes in either axis very well, but simple test signals of this type have problems in the case of a highly coupled rotorcraft model. It is generally accepted that doublets are not ideal as test inputs for helicopter identification although they may be useful when used in conjunction with other types of inputs [3]. To remove

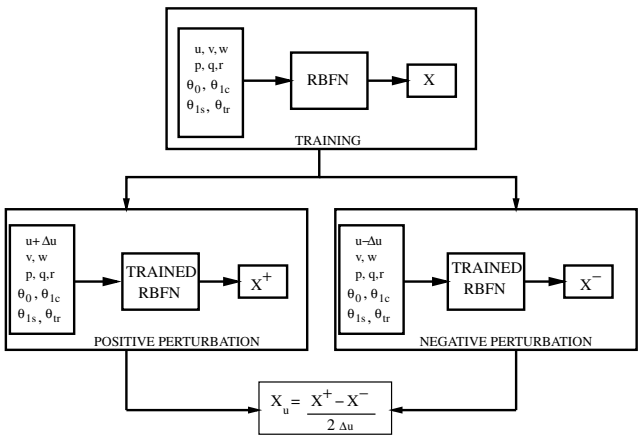

Fig. 12 X_u schematic representation of derivative computation using the delta method.

Table 4 Identification results: comparison between the delta method and 14-order model

Derivative	Delta method	14-order model [12]
X_u	−0.0340	−0.0352
X_w	−0.0709	−0.0992
Y_v	−0.1245	−0.1027
Y_p	−0.3419	1.3823
Z_u	−0.0185	−0.0067
Z_w	−0.2646	−0.2175
Z_p	−0.1257	−0.5669
L_u	−0.0833	−0.0059
L_v	−0.1393	−0.1080
L_w	−0.0861	−0.0683
L_q	0.7040	0.5287
M_u	−0.0161	−0.0081
M_v	0.0267	0.0281
M_w	−0.0181	−0.0196
M_p	−0.7393	−0.0906
N_u	−0.0086	−0.0039
N_v	0.0781	0.1276
N_w	0.0228	0.0141
N_p	−0.0784	0.2973
N_r	−1.0738	−0.8952

Table 5 Identification results: comparison between force derivatives with state variables by the delta method and 6-DOF model [3]. [AFDD: Aeroflightdynamics Directorate (U.S. Army), DLR: German Aerospace Center, NAE: National Aeronautical Establishment (Canada)]

Derivative	Delta method	AFDD	DLR	Glasgow	NAE
X_u	−0.0340	−0.0385	−0.059	−0.032	−0.050
X_v	−0.0190	0[a]	0[a]	0[a]	0.0043
X_w	−0.0709	−0.061	0.036	−0.0422	−0.017
X_p	0.4166	0.756	0[a]	0[a]	0.479
X_q	1.5740	2.548	0[a]	0[a]	1.206
Y_u	0.0307	0[a]	0[a]	0[a]	−0.061
Y_v	−0.1245	−0.221	−0.170	−0.131	−0.279
Y_w	−0.1356	−0.083	0[a]	0[a]	−0.0307
Y_p	−0.3419	−2.030	0[a]	0[a]	−2.993
Y_r	6.5181	0.950	1.332	0[a]	0.807
Z_u	−0.0185	0.2457	0.014	−0.0883	0.1016
Z_v	−0.1859	0[a]	0[a]	0[a]	−0.135
Z_w	−0.2646	−1.187	−0.998	−0.791	−1.106
Z_p	−0.1257	2.622	0[a]	0[a]	0.385

[a]Eliminated from model structure

drawbacks present in doublet inputs, a second form of multistate input, known as the modified 3211 input, was developed at the DLR, German Aerospace Center. The 3211 input excites a wide frequency band within a short period of time making it suitable for unstable and coupled systems [3,12]. Another form of pilot input known as the frequency sweep is also used in frequency-domain rotorcraft identification. The rotorcraft identification problem is difficult to solve using conventional time-domain techniques due to a high level of measurement noise and the presence of inter axis coupling [12,39,40]. Fu and Kaletka [12] used the modified 3211 input for identification and performed model validation using the frequency sweep input. Similarly, the present study uses data generated by the modified 3211 input for estimating the parameters. The same input signals used in [11] are used for identification to ensure a proper comparison of results.

Application of the RBFN-Based Delta Method to Flight Data

The flight data obtained by the DLR, German Aerospace Center are measured in terms of linear and angular accelerations. The data are converted to force and moment components for application to the RBFN by multiplying with the corresponding mass and moment of inertia values. The modified 3211 signal has a time length of 7 s.

Table 6 Identification results: comparison between moment derivatives with state variables by the delta method and 6-DOF model [3]

Derivative	Delta method	AFDD	DLR	Glasgow	NAE
L_u	−0.0833	−0.061	−0.081	−0.027	−0.099
L_v	−0.1393	−0.207	−0.271	−0.098	−0.270
L_w	−0.0861	0.168	0.116	0.130	0.116
L_p	−4.1502	−8.779	−8.501	−4.470	−1.895
L_q	0.7040	3.182	3.037	0[a]	4.454
L_r	0.9065	0.991	0.410	1.318	0.434
M_u	−0.0161	0[a]	0.029	0.0203	0.0078
M_v	0.0267	0.050	0.048	0[a]	0.0248
M_w	−0.0181	0.096	0.053	0.0491	0.0696
M_p	−0.7393	−0.998	−0.419	−1.367	−1.414
M_q	−2.3217	−4.493	−3.496	−2.217	−2.992
N_v	0.0781	0.082	0.117	0.0784	0.112
N_w	0.0228	−0.119	0.034	0.0281	−0.0634
N_p	−0.0784	−0.466	−1.057	−1.302	−0.692
N_r	−1.0738	−1.070	−0.858	−0.756	−1.017

[a]Eliminated from model structure

Table 7 Identification results: comparison between force derivatives with control variables by the delta method and 6-DOF model [3]

Derivative	Delta method	AFDD	DLR	Glasgow	NAE
X_{θ_0}	0.0319	−0.046	0[a]	0[a]	−0.0222
$X_{\theta_{1s}}$	−0.0268	−0.072	−0.028	−0.048	−0.05
$X_{\theta_{1c}}$	−0.0063	0[a]	0[a]	0[a]	−0.00176
Y_{θ_0}	−0.0309	−0.032	0[a]	0[a]	−0.0152
Z_{θ_0}	−0.2841	−0.388	−0.349	−0.259	−0.337
$Z_{\theta_{1s}}$	−0.1371	−0.103	−0.303	−0.140	−0.175

[a]Eliminated from model structure

Table 8 Identification results: comparison between moment derivatives with control variables by the delta method and 6-DOF model [3]

Derivative	Delta method	AFDD	DLR	Glasgow	NAE
$L\theta_0$	0.0130	0.058	0.032	0[a]	0.0142
$L_{\theta_{1s}}$	0.0243	0.073	0.024	0[a]	−0.005
$L_{\theta_{1c}}$	0.0392	0.179	0.185	0.0764	0.1361
M_{θ_0}	0.0292	0.073	0.057	0.039	0.048
$M_{\theta_{1s}}$	0.0470	0.098	0.093	0.0565	0.0787
$M_{\theta_{1c}}$	−0.017	0[a]	−0.009	0[a]	0.0106
N_{θ_0}	−0.0104	−0.051	0[a]	0[a]	−0.036
$N_{\theta_{1s}}$	−0.0436	−0.075	0[a]	0[a]	−0.051
$N_{\theta_{1c}}$	0.0318	0.033	0.026	0[a]	0.047

[a]Eliminated from model structure

Therefore, the parameters are extracted from the data generated for the first 7 s after application of the modified 3211 pilot control. The training data set is then prepared to train the RBFN. Unlike Raisinghani et al. [16], each state and control variable is included in the training of the RBFN in the present study. This is necessary for the mapping of coupling and cross axis effects present in the rotorcraft. The constituents of the training set are 1) u, v, w; 2) p, q, r; 3) θ_0, θ_{1c}, θ_{1s}, θ_{tr}; and 4) required force or moment component as output.

After selection of a training set for a particular stability or control parameter, the network is mapped for the given force or moment with the training variables. The input variable for which the derivative has to be computed is then given a perturbation. The rest of the variables are kept constant at their original values. The perturbation is made in both the positive and negative sides of the particular input variable. This results in two different data sets, one having a positively perturbed value of the selected state or control variable along with other constant variables and the other having a negatively perturbed value. These modified input data sets are now presented to the trained radial basis function network. The positive and negative perturbed data set gives the corresponding force or moment perturbed value. The RBFN parameters used in the computation are shown in Table 3.

Table 9 Identification results: verification of force derivatives using frequency sweep input

Derivative	3211	Frequency sweep
X_u	−0.0340	−0.0373
X_v	−0.0190	−0.0117
X_w	−0.0709	−0.0566
X_p	0.4166	1.09
X_q	1.5740	1.2188
Y_u	0.0307	0.0444
Y_v	−0.1245	−0.1143
Y_w	−0.1356	−0.1835
Y_r	6.5181	6.4246
Z_u	−0.0185	−0.0263
Z_v	−0.1859	−0.1987
Z_w	−0.2646	−0.3169

Table 10 Identification results: verification of moment derivatives using frequency sweep input

Derivative	3211	Frequency sweep
L_u	−0.0833	−0.0425
L_v	−0.1393	−0.0179
L_w	−0.0861	−0.0210
L_q	0.7040	2.4766
M_u	−0.0161	−0.0327
M_v	0.0267	0.0527
M_w	−0.0181	−0.0133
M_p	−0.7393	−0.5531
N_u	−0.0086	−0.004
N_v	0.0781	0.1326
N_w	0.0228	0.0376
N_p	−0.0784	−0.5635
N_r	−1.0738	−1.0872

The required derivative is then computed using the central difference formula. The process is illustrated in Fig. 12 by using the X_u derivative as an example when a longitudinal modified 3211 input is used as the pilot input. The steps are enumerated as:

1) The input file is made of all state and control variables.

2) The radial basis function network is then mapped with X force as output.

3) Two different modified input data sets having $u \pm \Delta u$ are made, keeping the other variables constant.

4) The data set having $u + \Delta u$ is presented to the previously trained network and the perturbed output is X^+.

5) Similarly, the data set having $u - \Delta u$ is presented to the trained network and the perturbed output is X^-.

6) The X_u derivative can now be computed as $[(X^+) - (X^-)]/2\Delta u$

7) The arithmetic mean of X_u computed at all time steps until 7 s is taken as the final result and is used for comparison with results obtained from conventional techniques.

The aforementioned methodology is used for computation of all the stability and control derivatives. The derivatives estimated using the RBFN-based delta method are compared to the derivatives from the 14-order model computed by Fu and Kaletka [12] in Table 4. The parameters estimated by using the RBFN-based delta method are in the same range as those obtained by the 9-DOF model. The computed stability and control parameters are also compared to the identified parameters of the BO 105 helicopter obtained by researchers at various organizations in Tables 5–8 [3]. It can be seen from Tables 5–8 that the RBFN-based delta method is able to estimate most of the stability and control parameters satisfactorily. Because rotorcraft parameter identification from flight-test data is a very complicated problem, there is considerable variation in the prediction of different researchers.

Table 11 Identification results: verification of control derivatives using frequency sweep input

Derivative	3211	Frequency sweep
X_{θ_0}	0.0319	0.0304
$X_{\theta_{1s}}$	−0.0268	−0.0237
Y_{θ_0}	−0.0309	−0.0407
Z_{θ_0}	−0.2841	−0.3778
$Z_{\theta_{1s}}$	−0.1371	−0.094
L_{θ_0}	0.0130	0.0172
$L_{\theta_{1s}}$	0.0392	0.583
$L_{\theta_{1c}}$	0.0243	0.0208
M_{θ_0}	0.0292	0.0317
$M_{\theta_{1s}}$	0.0470	0.0545
$M_{\theta_{1c}}$	−0.0107	−0.0093
$N_{\theta_{1c}}$	0.0318	0.0271

Verification is an important step in the system identification process. Fu and Kaletka [12] pointed out that verification should always be conducted with data not used in identification. Therefore, flight-test data from frequency sweeps are used for the verification. Tables 9–11 compare selected estimated derivatives from modified 3211 and frequency sweep pilot control inputs. There is good agreement in direct and coupled stability derivatives demonstrating the predictive capability of the RBFN-based delta method.

Finally, we point out that the RBFN approach is philosophically different from the other classical system identification approaches. The RBFN-based delta method is model free and therefore provides a useful tool for rotorcraft parameter identification from flight-test data. RBFN-based derivatives can also be used to compare derivatives evaluated using the conventional system identification techniques as an alternative computational method.

Conclusions

A new technique for rotorcraft parameter estimation based on the RBFN-based delta method is proposed. This technique does not require any mathematical modeling or conventional parameter estimation techniques for identification from flight data. The method is first tested on simulated data generated by a nonlinear simulation model. Both ideal (noise free) and noise contaminated data are considered. Also, both state and measurement noise are considered. Then the established methodology is used for the computation of the stability and control derivatives directly from the real time flight-test flight data of a BO 105 helicopter. The following conclusions are drawn from the study:

1) The RBFN is able to successfully map the coupling and nonlinearities in the system and estimate satisfactory stability and control derivatives using the delta method, both for simulated ideal and noisy data.

2) The RBFN-based delta method is not greatly affected by the type of noise present in the data. The performance is satisfactory in the case of state and measurement noise.

3) The delta method is satisfactorily able to identify the parameters from flight data and results have about the same level of accuracy as a 14-order model.

4) The RBFN-based delta method is found to give satisfactory results in the case of a lesser number of data points. This helps in parameter estimation when the number of data points obtained from flight tests are fewer.

5) The parameter estimation using the RBFN has acceptable predictive capability as the verification results by frequency sweep input are in the same range as those estimated using the modified 3211 input.

6) The RBFN approach provides an alternative to the conventional parameter identification approach when a mathematical model is not available. It can also be used as a method that gives an estimate of the derivatives, which can be used to guide conventional parameter estimation work and model development.

Acknowledgments

The authors thankfully acknowledge R. Jategaonkar and W. V. Gruenhagen of DLR, German Aerospace Center, for providing the BO 105 flight data. We are also grateful to the Aeronautical Research and Development Board (ARDB), Government of India, for the funding and facilities provided for this project.

References

[1] Prouty, R. W., *Helicopter Performance, Stability, and Control*, Krieger, Malabar, FL, 1986.

[2] Padfield, G. D., *Helicopter Flight Dynamics: The Theory and Application of Flying Qualities and Simulation Modeling*, AIAA Education Series, AIAA, Reston, VA, 1999.

[3] AGARD, "Rotorcraft System Identification," AGARD AR 280, LS 178, 1991.

[4] Jategaonkar, R. V., Fischenberg, D., and Gruenhagen, W. V., "Aerodynamic Modeling and System Identification from Flight Data - Recent Applications at DLR," *Journal of Aircraft*, Vol. 41, No. 4, 2004, pp. 681–691.

[5] Jategaonkar, R. V., *Flight Vehicle System Identification: A Time Domain Methodology*, AIAA Education Series, AIAA, Reston, VA, 2006.

[6] Tishler, M. B., and Remple, R. K., *Aircraft and Rotorcraft System Identification: Engineering Methods With Flight-Test Examples*, AIAA Education Series, AIAA, Reston, VA, 2006.

[7] Hamel, P. G., and Kaletka, J., "Advances in Rotorcraft System Identification," *Progress in Aerospace Sciences*, Vol. 33, No. 3–4, 1997, pp. 259–284. doi:10.1016/S0376-0421(96)00005-X

[8] Hamel, P. G., and Jategaonkar, R. V., "Evolution of Flight Vehicle System Identification," *Journal of Aircraft*, Vol. 33, No. 1, 1996, pp. 9–28.

[9] Morelli, E. A., and Klein, V., "Application of System Identification to Aircraft at NASA Langley Research Center," *Journal of Aircraft*, Vol. 42, No. 1, 2005, pp. 12–25.

[10] Iliff, K. W., and Maine, R. E., "More Than You May Want to Know About Maximum Likelihood Estimation," NASA TM 85905, 1985.

[11] Iliff, K. W., and Maine, R. E., "Application of Parameter Estimation to Aircraft Stability and Control the Output Error Approach," NASA RP 1168, 1986.

[12] Fu, K. H., and Kaletka, J., "Frequency Domain Identification of BO 105 Derivative Models with Rotor Degrees of Freedom," *Journal of the American Helicopter Society*, Vol. 38, No. 1, 1993, pp. 73–83.

[13] Pavel, M., "On the Necessary Degrees of Freedom for Helicopter and Wind Turbine Low-Frequency Mode Modeling," Ph.D. Thesis, Technische Universiteit Delft, Delft, The Netherlands, 2001.

[14] Raol, J. R., and Jategaonkar, R. V., "Aircraft Parameter Estimation Using Recurrent Neural Networks—A Critical Appraisal," AIAA Paper 95-3504, 1995.

[15] Raisinghani, S. C., Ghosh, A. K., and Kalra, P. K., "Two New Techniques for Parameter Estimation Using Neural Networks," *The Aeronautical Journal*, Vol. 102, No. 1011, 1998, pp. 25–29.

[16] Raisinghani, S. C., Ghosh, A. K., and Khubchandani, S., "Estimation of Aircraft Lateral-Directional Parameters Using Neural Networks," *Journal of Aircraft*, Vol. 35, No. 6, 1998, pp. 876–881.

[17] Vijaykumar, M., Omkar, S. N., Ganguli, R., Sampath, P., and Suresh, S., "Identification of Helicopter Dynamics Using Recurrent Neural Networks and Flight Data," *Journal of the American Helicopter Society*, Vol. 51, No. 2, 2006, pp. 164–174.

[18] Kim, B. S., and Calise, A. J., "Nonlinear Flight Control Using Neural Networks," *Journal of Guidance, Control, and Dynamics*, Vol. 20, No. 1, 2005, pp. 26–33.

[19] Suresh, S., Omkar, S. N., Mani, V., and Sundararajan, N., "Nonlinear Adaptive Neural Controller for Unstable Aircraft," *Journal of Guidance, Control, and Dynamics*, Vol. 28, No. 6, 2005, pp. 1103–1111.

[20] Suresh, S., Omkar, S. N., Mani, V., and Sundararajan, N., "Direct Adaptive Neural Flight Controller for F-8 Fighter Aircraft," *Journal of Guidance, Control, and Dynamics*, Vol. 29, No. 2, 2006, pp. 454–464.

[21] Amin, S. M., Gerhart, V., and Rodin, E. Y., "System Identification via Artificial Neural Networks—Applications to On-line Aircraft Parameter Estimation," AIAA Paper 1997-5612, 1997.

[22] Habib, S., and Zaghloul, M. E., "System Identification Using Time Dependent Neural Networks—A Simpler Approach," AIAA Paper 1996-3803, 1996.

[23] Tsou, P., and Shen, M. H. H., "Structural Damage Detection and

Identification Using Neural Networks," *AIAA Journal*, Vol. 32, No. 1, 1994, pp. 176–183.

[24] Reddy, R. R. K., and Ganguli, R., "Structural Damage Detection in a Helicopter Rotor Blade Using Radial Basis Function Neural Networks," *Smart Materials and Structures*, Vol. 12, No. 2, 2003, pp. 232–241. doi:10.1088/0964-1726/12/2/311

[25] Ganguli, R., Chopra, I., and Haas, D. J., "Detection of Helicopter Rotor System Simulated Faults Using Neural Networks," *Journal of the American Helicopter Society*, Vol. 42, No. 2, 1997, pp. 161–171.

[26] Ganguli, R., Chopra, I., and Haas, D. J., "Helicopter Rotor System Fault Detection Using Physics-Based Model and Neural Networks," *AIAA Journal*, Vol. 36, No. 6, 1998, pp. 1078–1086.

[27] Malaek, S. M. B., and Izadi, H. A., "Progressive Certification Process Based on Living Systems Architecture Using Learning Capable Controllers," *Journal of Aircraft*, Vol. 43, No. 1, 2006, pp. 207–215.

[28] Ogretim, E., Huebsch, W., and Shinn, A., "Aircraft Ice Accretion Prediction Based on Neural Networks," *Journal of Aircraft*, Vol. 43, No. 1, 2006, pp. 233–240.

[29] Al-Garni, A. Z., Jamal, A., Ahmad, A. M., Al-Garni, A. M., and Tozan, M., "Failure-Rate Prediction for De Havilland Dash-8 Tires Employing Neural Network Technique," *Journal of Aircraft*, Vol. 43, No. 2, 2006, pp. 537–543.

[30] Sahani, N. A., Horn, J. F., Jeram, G. J. J., and Prasad, J. V. R., "Hub Moment Limit Protection Using Neural Network Prediction," *Journal of the American Helicopter Society*, Vol. 51, No. 4, 2006, pp. 331–340.

[31] Horn, J., Calise, A. J., and Prasad, J. V. R., "Flight Envelope Limit Detection and Avoidance for Rotorcraft," *Journal of the American Helicopter Society*, Vol. 47, No. 4, 2002, pp. 253–262.

[32] Kottapalli, S., "Neural Network Modeling of UH-60A Pilot Vibration," *Journal of the American Helicopter Society*, Vol. 51, No. 2, 2006, pp. 195–201.

[33] Horni, K. K., Stinchcombe, M., and White, H., "Multi-Layer Feed Forward Networks Are Universal Approximaters," *Neural Networks*, Vol. 2, No. 5, 1989, pp. 359–368. doi:10.1016/0893-6080(89)90020-8

[34] Suresh, S., Omkar, S. N., Ganguli, R., and Mani, V., "Identification of Crack Location and Depth in a Cantilever Beam Using a Modular Neural Network Approach," *Smart Materials and Structures*, Vol. 13, No. 4, 2004, pp. 907–915. doi:10.1088/0964-1726/13/4/029

[35] Park, J. W., Harley, R. G., and Venayagamoorthy, G. K., "Comparison of MLP and RBF Neural Networks Using Deviation Signals for On-Line Identification of a Synchronous Generator," *IEEE Power Engineering Society Winter Meeting*, Vol. 1, IEEE Press, Washington, D.C., 2002, pp. 274–279.

[36] Baraldi, A., Blonda, P., Satalino, G., D'Addabbo, A., and Tarantino, C., "RBF Two Stage Learning Networks Exploiting Supervised Data in the Selection of Hidden Unit Parameters; An Application to SAR Data Classification," *Proceedings in IGARSS*, IEEE Press, Washington, D.C., 2000, pp. 672–674.

[37] Kumar, R., Omkar, S. N., and Ganguli, R., "Computation of Rotorcraft Aerodynamic Derivatives Using Neural Networks," *Heli-Japan 2006 AHS International Meeting on Advance Rotorcraft Technologies and Life Saving Activities*, Nagoya, Aichi Prefecture, Japan, 15–17 Nov. 2006, pp. T213-2-1–T213-2-17.

[38] Haykin, S., *Neural Networks: A Comprehensive Foundation*, Macmillan, New York/Indianapolis, IN, 1994.

[39] Padfield, G. D., "A Theoretical Model of Helicopter Flight Mechanics for Application to Piloted Simulation," RAE Tech Report 81048, 1981.

[40] Tischler, M. B., and Cauffman, M. G., "Frequency-Response Method for Rotorcraft System Identification: Flight Applications to BO 105 Coupled Rotor/Fuselage Dynamics," *Journal of the American Helicopter Society*, Vol. 37, No. 3, 1992, pp. 3–17.